Struct Multidisc Optim (2009) 38:535–543
DOI 10.1007/s00158-008-0317-5

RESEARCH PAPER

Topology optimization with design-dependent pressure loading

Bin Zheng · Ching-jui Chang · Hae Chang Gea

Received: 29 January 2008 / Revised: 4 September 2008 / Accepted: 7 September 2008 / Published online: 14 October 2008

Abstract In this paper, the layout of structures under design-dependent pressure loading is optimized using a topology optimization approach. In contrast to topology optimization problems with conventional static external loading, the position and direction of pressure loading are changing with topology of structure during optimization iterations. In order to model the changing structural surface boundaries under design-dependent pressure loading, a pseudo equal-potential function is introduced. Design sensitivity analysis is derived from the adjoint method. Three examples solved by the proposed method are presented.

Keywords Topology optimization · Design-dependent loading · Pressure loading

1 Introduction

Since the homogenization method was first introduced by Bendsøe and Kikuchi (1988) in solving topology optimization problems, various forms of topology optimization methods have been successfully developed and applied to various structure design problems. Topology optimization of Linear elastic plane structures for the stiffest design was studied by Suzuki and Kikuchi (1991) using the homogenization method. Diaz and Bendsøe (1992) extended topology optimization to multiple load design. The optimal stiffener design of shell/plate structures with small deformation was studied by Luo and Gea (1998). Topology optimization for elastic structures considering vibration behavior was considered by Pedersen (2000), Chen and Wu (1998), Gea and Fu (1997), Du and Olhoff (2007). Local stress constraints of continuum structures was included in the topology optimization formulation by Duysinx and Bendsøe (1998). Topology optimization for both geometrically and materially nonlinear problems was studied by Jung and Gea (2004). The level set method was used to in some topology optimization problems by Allaire et al. (2004) and Wang et al. (2004). An extensive literature survey can be found in Bendsøe and Sigmund (2004).

Traditionally, topology optimization starts with a predefined design domain and boundary conditions which include supports and applied loading. The design domain and boundary conditions are invariant with respect to the solution during the iterative optimization process. In engineering practice, exact boundary conditions sometimes cannot be defined completely before the final design is identified; in other words, these boundary conditions are design dependent. However, conventional topology optimization methods cannot proceed under the design dependent boundary conditions. Literatures on the design dependent topology optimization method are very limited comparing to design independent topology optimization method. The first solution for design dependent loads problem is "Prager structures" proposed by Rozvany and Prager (1979). Topology optimization with design dependent supports for multiple components was studied by Chickermane

B. Zheng
School of Mechatronics Engineering,
University of Electronic Science and Technology of China,
Chengdu 610054, China

C.-j. Chang · H. C. Gea (✉)
Department of Mechanical and Aerospace Engineering,
Rutgers University, Piscataway, NJ 08854, USA
e-mail: gea@rutgers.edu

and Gea (1997). Chen and Kikuchi (2001) simulated the design dependent pressure loading by applying fictitious thermal loading between fluid and non-fluid regions in which the elements had different coefficients of thermal expansion, and used a "dryness coefficient" to distinguish between these two regions. Hammer and Olhoff (2002) studied topology optimization with design dependent pressure loading by forming new pressure surfaces along iso-volumetric density surfaces using spline functions during every iteration. Du and Olhoff (2004a, b) further improved this method by using two techniques: one is to identify the iso-volumetric density surfaces by using the material density information in both current iteration and previous one; another technique is to directly calculate the sensitivity of loads by using finite different method. Fuchs and Shemesh (2004) introduced high order curve parameters, which were independent of density distribution, to define the loading surface on water pressured problems. As an alternative approach, Yang et al. (2005) applied evolutionary methods for topology optimization problems with design dependent loads. Bourdin and Chambolle (2003) introduced a three-phase material (void/fluid/solid) model and used the fluid phase to exert the pressure force on its interface with the solid phase. Sigmund and Clausen (2007) defined the void phase to be an impressible hydrostatic fluid and then the pressure load is no longer design dependent at the expense of increasing the number of design variables.

In this paper, a new approach for topology optimization with design dependent pressure loading is presented. In this new approach, a potential function, which is dependent of density distribution, is created to define the design dependent loading surface. In order to regenerate pressure loads, a new transmission coefficient H_i for each element is introduced to distinguish the pressure transmissible region from non-transmissible region. Sensitivity of design dependent pressure load can evaluated easily with the aid of the transmission coefficient. The remainder of this paper is organized as follows: The topology optimization problem formulation of design dependent pressure loading is described in the next section. Then, design dependent pressure loading is modeled by a potential function and its sensitivity analysis is derived. Finally, three examples solved by the proposed method are presented.

2 Problem formulation

In a conventional topology optimization formulation, applied loading is kept as invariant even when structural topology changes during iterations. However, in a design dependent structural topology optimization problem, positions and directions of applied loading will vary with different structural topology during optimization processes. A schematic representation of two designs with design dependent loading during optimization iteration is shown in Fig. 1. As shown in Fig. 1, the external force of the original design at the left hand side changes its location and direction under a different structural layout in the right hand side. The dashed design at the right hand side represents the original layout.

In this paper, our focus is on the modeling of the moving boundary condition of design dependent pressure loading. Therefore, the simplest formulation, the minimal mean compliance design, is used. The design objective is to minimize the mean compliance C under a constant volume of material constraint $\bar{V}$:

$$\begin{aligned} &\min_x \ C \\ &\text{s.t. } V(x) = \int_\Omega x \, d\Omega \ \le \bar{V} \\ &\quad 0 < x < 1 \end{aligned} \tag{1}$$

where design variable x defines the relative material volume density distribution in design domain. The relationship between material properties and design variable x follows the spherical micro-inclusion model in Gea (1996). The compliance C of a structure is defined as

$$C = \int_{\Gamma_F} \mathbf{Fu} \, d\Gamma_p \,, \tag{2}$$

where $\mathbf{u}$ is the displacement field. Under the Finite Element format, this equation is expressed as

$$C = \mathbf{U}^T \mathbf{K} \mathbf{U} \,, \tag{3}$$

where $\mathbf{K}$ is the stiffness matrix, $\mathbf{U}$ is the displacement vector.

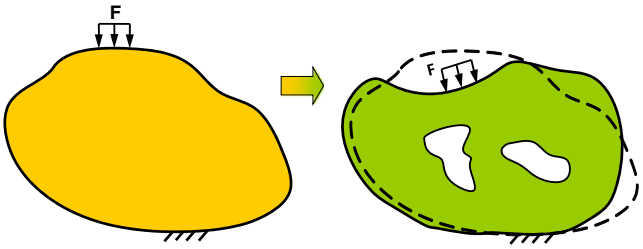

Fig. 1 A schematic representation of design dependent loads

3 Design dependent pressure loading

Although the pressure maintains as a constant during topology optimization process, the applied loads at the boundary surface may not. As the material distribution pattern changes, the pressure loading surface will change accordingly. Therefore, the most challenging task of modeling the design dependent loading is to define the relationship between the material distribution and the varying pressure loading surface. In this paper, a potential function which is based on the electric potential is used to model the pressure loading boundary. To demonstrate this concept, only two-dimensional objects are studied in this paper. In a two-dimensional model, the surface where the pressure loading acts upon is a curve, and the direction of pressure loading should always be normal to this curve. In following subsections, we will discuss the definition of loading surface using a potential function and the representation of the equivalent nodal forces for finite element analysis.

3.1 Definition of the loading surface

The basic concept of the proposed method is to find a pseudo equal-potential curve in order to model the loading surface. We use the word "pseudo" here is because we assume that the material in the design domain is fictitious isotropic insulator and we apply a fictitious electric field on the design domain. A simple example about the applied fictitious electric field is shown in Fig. 2. An electric potential ϕ_0 is applied to the boundary where the initial pressure $\mathbf{P}_0$ acts on; the electric ground is applied to the surface of supports. For this kind of electrostatic problem, the relationship between the potential ϕ and the charge density ρ can be derived from Maxwell's equations as:

$$\nabla^2\phi + \frac{\rho}{\epsilon} = 0 \ . \tag{4}$$

This partial differential equation can be transformed into a linear algebra expression as:

$$\mathbf{D} = -\varepsilon\mathbf{E} \ , \tag{5}$$

where $\mathbf{D}$ and $\mathbf{E}$ are the electric displacement vector and electric field vector, respectively; ε is the diagonal dielectric matrix. In our work, the relationship between the density of the material x and the dielectric permittivity constant ϵ is set as

$$\epsilon = \frac{1}{x^m} \ , \tag{6}$$

where m presents a penalty factor that is chosen as 2 in this study. Based on (5), the electrostatic finite element format can be established as

$$\mathbf{K}_\varphi \Phi \ = \ Q \ , \tag{7}$$

where $\mathbf{K}_\varphi$ is a dielectric permittivity related matrix, and Q is a vector related to electric charge. Then, electric potential distribution Φ in the entire design domain can be calculated by finite element method.

The fictitious electric field acting on the design domain and the fictitious dielectric permittivity property pave a path to define the pressure load surface. The divergent of electric field strength ($-\vec{\nabla}\phi$ or $\mathbf{E}$) is proportional to x^m from (4) and (6). This implies that the voids in the design domain, where the density is near zero, do not change the potential values. In Fig. 2b, the relationship between the material distribution pattern and positions of equal potential curves Γ_ϕ is shown.

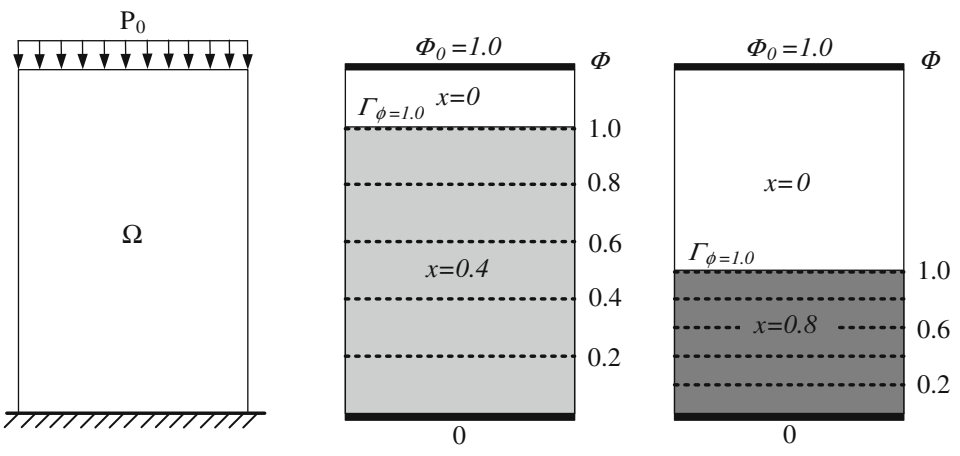

(a) Design domain (b) Equal potential curves for two different density distributions

Fig. 2 Representation of loading surface (**a**, **b**)

The electric potential $\phi_0 = 1.0$ is applying on the upside boundary and potential 0 is applying on the underside boundary. The dash curves represent several equal potential curves, and their potential value ϕ are listed on the right side of the design domain. Although their mass distribution patterns are different in these two design domains of Fig. 2b, decreases of potential across the void region ($x = 0$) are the same for both patterns, equal to zero. It seems that ϕ_0 is applied on the equal potential curve $\Gamma_{\phi=1.0}$, and all materials used to design are in the gray area under the curve of $\Gamma_{\phi=1.0}$. As we mentioned before, the lower bound of design variable x_{min} is a little greater than zero, hence the criterion electric potential is set as $\phi_c = 0.95\phi_0$ in our study. The equal potential curve Γ_{ϕ_c} divides the design domain into two regions: one region has nearly all design material and the other only has a very little material. Therefore, it is used to represent the pressure loading surface.

3.2 Representation of the equivalent nodal forces

In this paper, a simple method is proposed to generate equivalent nodal forces based on the potential information calculated from (7). First, a transmission coefficient H_i is defined as follows:

$$H_i(\bar{\phi}_i) = \begin{cases} 0 & \text{if } \bar{\phi}_i \le \phi_c - \Delta \\ \frac{(\bar{\phi}_i - (\phi_c - \Delta))^2}{2\Delta^2} & \text{if } \phi_c - \Delta < \bar{\phi}_i \le \phi_c \\ 1 - \frac{(\bar{\phi}_i - (\phi_c + \Delta))^2}{2\Delta^2} & \text{if } \phi_c < \bar{\phi}_i \le \phi_c + \Delta \\ 1 & \text{if } \phi_c + \Delta < \bar{\phi}_i \end{cases}, \quad (8)$$

where ϕ_c is the predetermined potential criterion; Δ represents the transition interval; $\bar{\phi}_i$ is the average potential of the i^{th} finite element with n nodes,

$$\bar{\phi}_i = \frac{1}{n} \sum_{j=1}^{n} \phi_{ij} \,. \quad (9)$$

The sketch of the transmission coefficient is shown in Fig. 3a. For computational convenience, we reduced the transition interval Δ to a very small value so that the instance of the average potential within the transition interval becomes very rare. Although the final form of transmission coefficient is very similar to a Heaviside function as shown in Fig. 3b, it is worth noting that the transmission coefficient is always continuous and differentiable. This differentiability is necessary for sensitivity analysis and gradient based optimization in our approach. In very rare cases, the element average potential may still fall within the transition interval, $(\phi_c - \Delta, \phi_c + \Delta)$ and the first derivative of the transmission coefficient will become very large. To reduce the numerical complication, a small value of potential is added to its average potential in order to bring it outside the transition interval. Since the modification is very minor, it will not affect the final results at all. In this way, there are only two possible values, either 0 or 1, of transmission coefficient will be assigned to each element. Finite element cells whose transmission coefficients as $H_i = 1$ comprise the pressure transmissible region Ω_p; all other cells comprise non-transmissible region Ω_n. Then, the pressure loading surface Γ_{ϕ_c} is formed by the zigzag boundary lying between these two regions.

The next step is to generate equivalent nodal forces at the nodes along the new zigzag loading surface. Since the loading surface has been identified. For all adjacent elements of the loading surface, we assign the element inner pressure as $P_0 H_i$. This means the pressure in the i^{th} element is P_0 if the element is in the pressure transmissible region Ω_p and the pressure is 0 if it is in the non-transmissible region Ω_n. The nodal force of each element can then be obtained from a simple conversion from the pressure loading at the boundary with a direction normal to the boundary. A sketch of pressure load and its equivalent nodal forces in a part

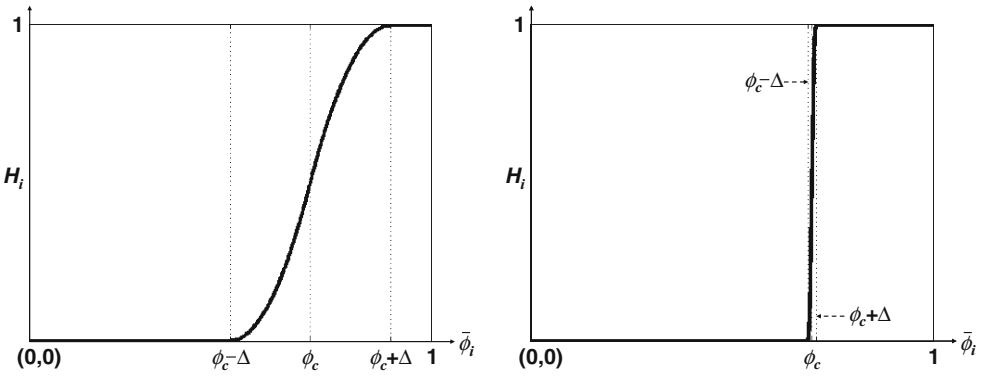

(a) Transmission coefficient (b) Transmission coefficient with very small Δ

Fig. 3 Transmission coefficient with different Δ (**a**, **b**)

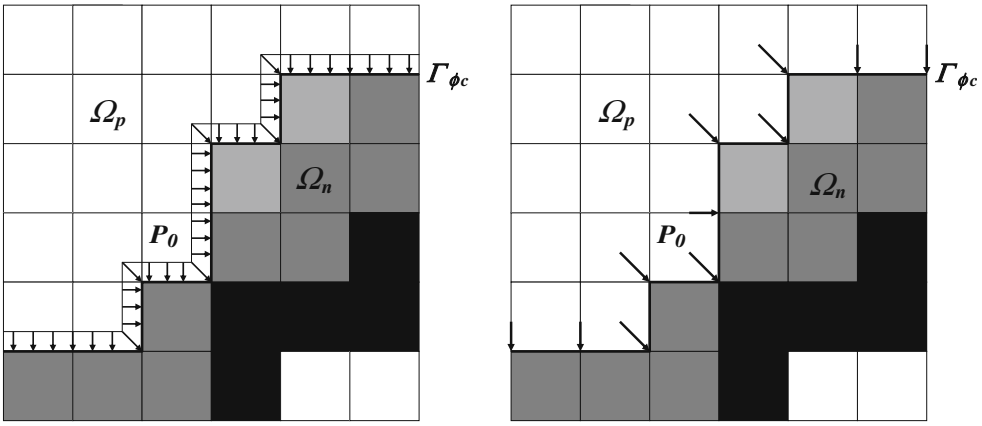

Fig. 4 A sketch of pressure load and its equivalent forces (**a**, **b**)

(a) Pressure load (b) Equivalent forces

of design domain are shown in Fig. 4. The equivalent nodal forces are zero for all nodes in region Ω_p or Ω_n and only the nodes on surface Γ_{ϕ_c} have nonzero equivalent nodal forces.

4 Sensitivity analysis

Sensitivity information is needed for a gradient based search method. In this study, the adjoint method is used to derive the sensitivity of mean compliance C in (3). More details of the adjoint method can be found in Tortorelli and Michaleris (1994). First, A new function C^* is defined as

$$C^* = \mathbf{U}^T\mathbf{K}_u\mathbf{U} + \lambda^T(\mathbf{K}_u\mathbf{U} - \mathbf{F}) \tag{10}$$

where λ is an arbitrary adjoint displacement vector , $\mathbf{U}$ and $\mathbf{F}$ are vectors of displacement and external force, respectively; $\mathbf{K}_u$ is the global stiffness matrix. This new function is the same as objective function C because the equilibrium of a discrete model can be expressed as $\mathbf{K}_u\mathbf{U} = \mathbf{F}$, and it makes the term $\lambda^T(\mathbf{K}_u\mathbf{U} - \mathbf{F})$ always be zero. Then, the sensitivity of C^* with respect to the design variables x_i can be written as

$$\frac{\partial C^*}{\partial x_i} = (\mathbf{U} + \lambda)^T\frac{\partial \mathbf{K}_u}{\partial x_i}\mathbf{U} + (2\mathbf{U} + \lambda)^T\mathbf{K}_u\frac{\partial \mathbf{U}}{\partial x_i} - \lambda^T\frac{\partial \mathbf{F}}{\partial x_i} \tag{11}$$

By setting the adjoint vector $\lambda = -2\mathbf{U}$ into (11), it gives

$$\frac{\partial C^*}{\partial x_i} = -\mathbf{U}^T\frac{\partial \mathbf{K}_u}{\partial x_i}\mathbf{U} + 2\mathbf{U}^T\frac{\partial \mathbf{F}}{\partial x_i} \quad . \tag{12}$$

The first term at the RHS of (12) is easy to be evaluated as a conventional topology optimization approach. Therefore, our attention is at the second term, the first

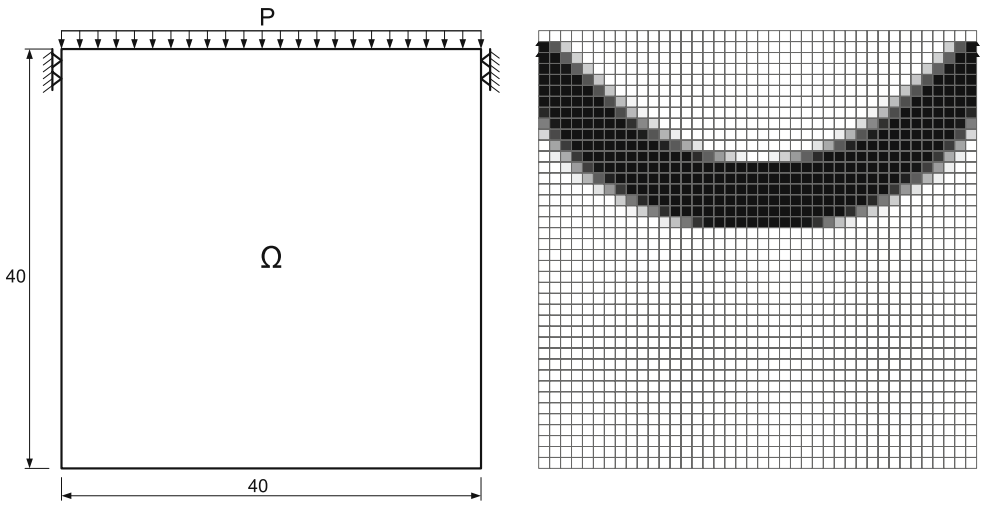

Fig. 5 Structure under design dependent pressure loading supported at top corners (**a**, **b**)

(a) Design domain (b) Optimized structure

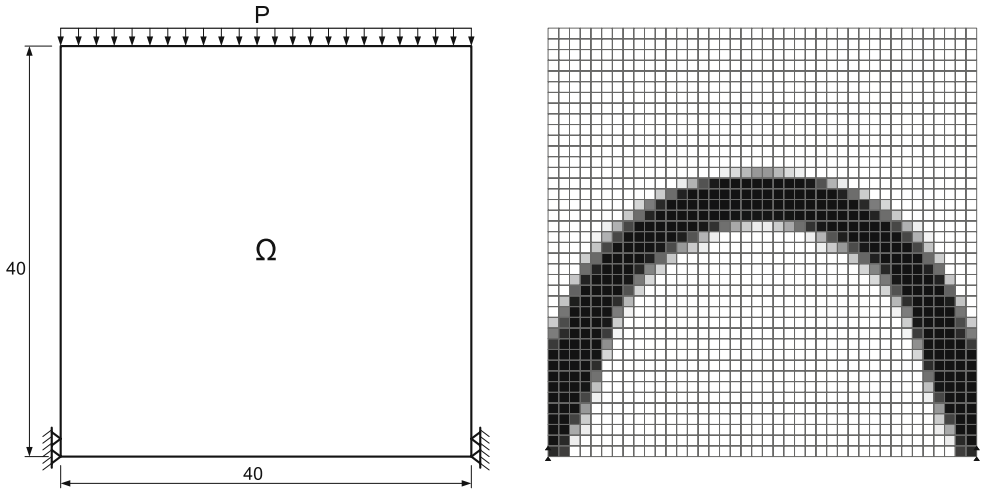

(a) Design domain (b) Optimized structure

Fig. 6 Structure under design dependent pressure loading supported at bottom corners (**a**, **b**)

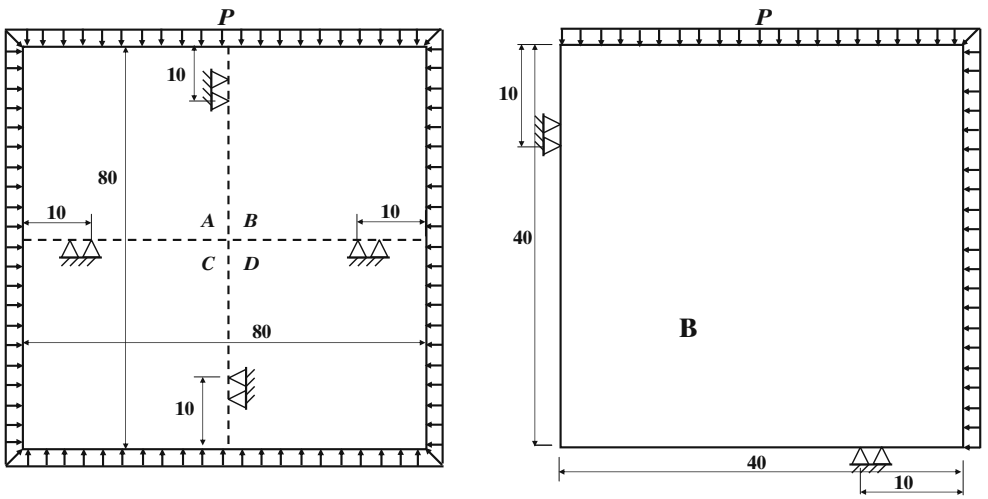

(a) Design domain (b) Sub-design domain at part B

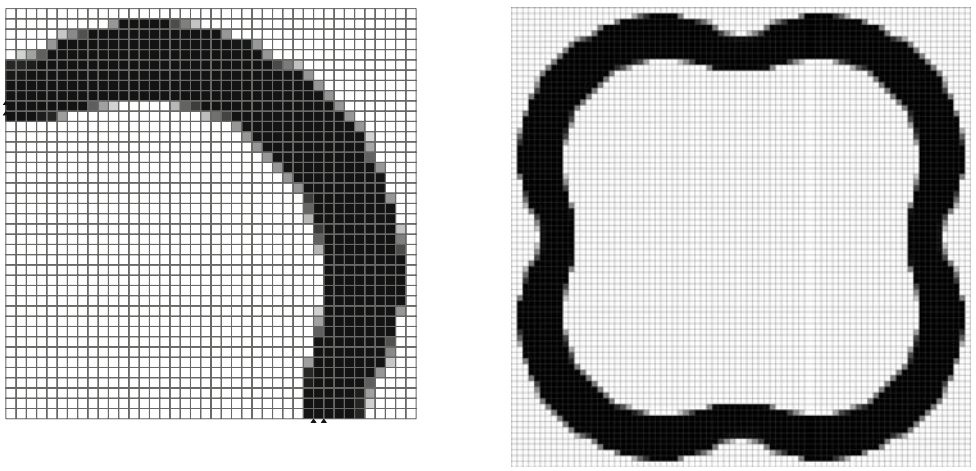

(c) Optimized structure at part B (d) Optimized structure

Fig. 7 Structure with four supports under hydrostatic pressure (**a**–**d**)

derivative of external force, **F**. As we discussed before, external force **F** is converted from element inner pressure that is a function of the transmission coefficient, H_i and the first derivative of the transmission coefficient is zero almost everywhere except within the transition interval $(\phi_c - \Delta, \phi_c + \Delta)$. Furthermore, the transition interval Δ is reduced to a very small value and a small potential has been added to the elements with their average potentials inside the transition interval. Therefore, the first derivative of all usable transmission coefficient is always zero and the first derivatives of external force in (12) vanish. Once the sensitivity analysis is completed, the topology optimization problem under design dependent loads is solved by a Generalized Convex Approximation method (Chickermane and Gea 1996).

5 Numerical examples

5.1 Example 1

In the first example, a structure subject to a pressure from the top is optimized. The structure is clamped at two top corners where marked as the triangles as shown in Fig. 5a. The pressure load is comes from the top, and is restricted to act on the equal potential curve of $\phi_c = 0.95\phi_0$ in every optimization iteration. The total available solid region is limited to 20% of the total volume in the design domain. The finite element analysis model consists of 40 by 40 elements. The optimized structure of this model is shown in Fig. 5b. It is an inverted arch, and a similar structure was obtained in the Hammer and Olhoff's work (2002).

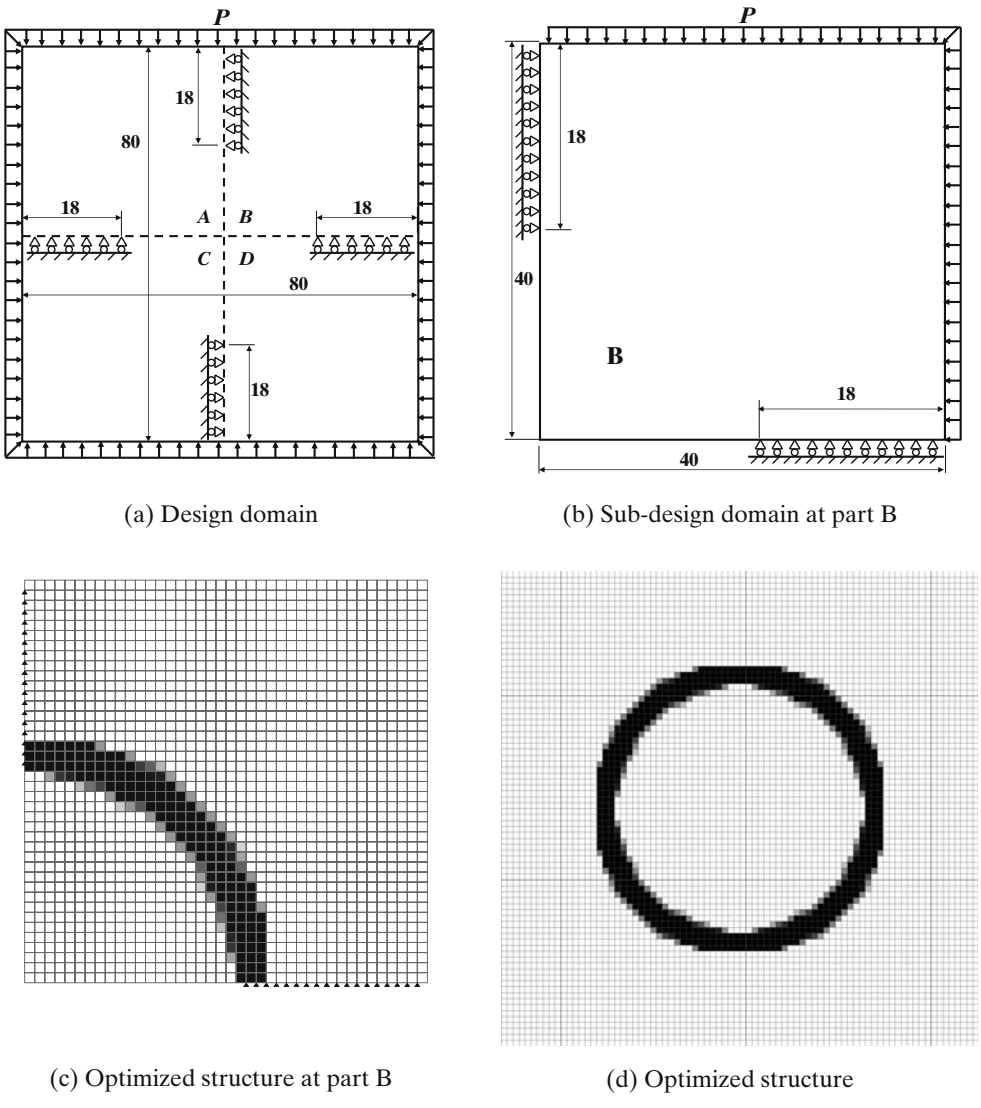

(a) Design domain

(b) Sub-design domain at part B

(c) Optimized structure at part B

(d) Optimized structure

Fig. 8 Structure with four sliding supports under hydrostatic pressure (**a**–**d**)

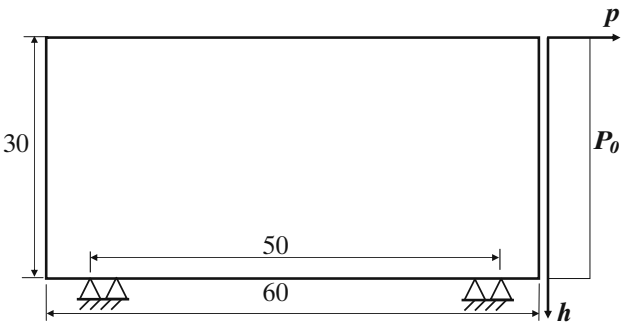

(a) Finite element model

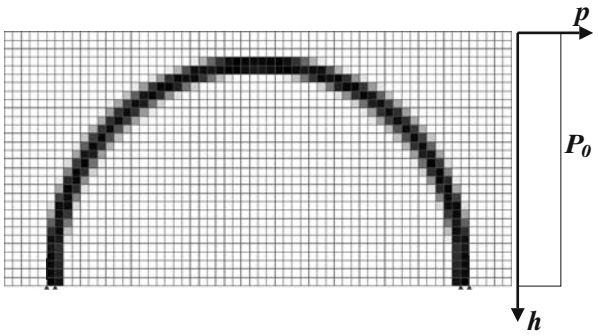

(b) Optimized structure

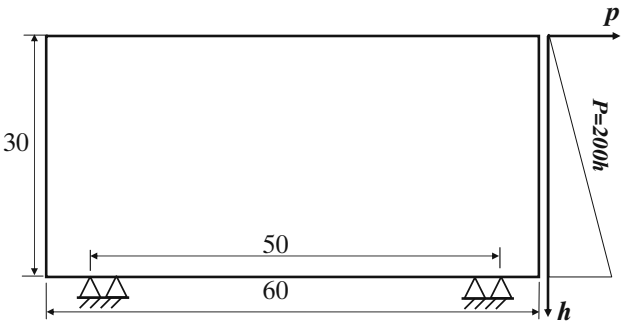

(c) Finite element model

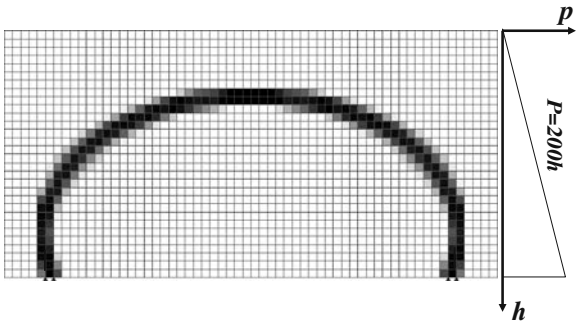

(d) Optimized structure

Fig. 9 Depth varying pressure loading structures (**a**–**d**)

When the supports are moved to the lower corners, as shown in Fig. 6a, the optimized structure, which is shown in Fig. 6b, is an arch which spans the two supports.

5.2 Example 2

Consider a structure surrounding by hydrostatic pressure load with four supports at each side as shown in Fig. 7a. Since this model is symmetric, we only use 1/4 of the entire model with symmetric boundary conditions to be the design domain as shown in Fig. 7b. The upper limit of available solid areas is 30% of the total volume in the design domain. The optimized structure of a quarter model is shown in Fig. 7c and the optimized structure of the whole design domain is shown in Fig. 7d.

Instead of fixed locations for supports, supports are replaced with four roller support lines as shown in Fig. 8a. The solid region is limited to 10% of the total volume in the design domain. The optimized structures of the quarter model and the complete model are shown in Fig. 8c and Fig. 8d. This example demonstrates that the supporting condition can also be design dependent under this formulation.

5.3 Example 3

The method proposed in the paper can be also used in the depth varying pressure load structures. Two pressure loading patterns with the same dimensions and positions of fixed points are shown in Fig. 9a and Fig. 9c. The design-dependent pressure load of the first model is the same along with the depth h while that of the second model increases 200N/unit linearly with the depth h. The solid area is limited to 10% of the total volume in the design domain. Optimized structures are shown in Fig. 9b and Fig. 9d, the first one is half of a circle and the second one is half of an oval shape.

6 Conclusion

Topology optimization problems with design-dependent pressure loadings are studied in this paper. The most challenging task of modeling the design dependent pressure loading is to define the relationship between the material distribution and the varying pressure loading surface. In this paper, a potential

function that is based on the electric potential and a transmission coefficient are used to define the pressure loading boundary and the equivalent nodal forces are then represented as a function of transmission coefficients. By tightening the transition interval of transmission coefficient and applying a small modification on the average potential, we have two advantages: pressure loading boundary can be clearly identified and the sensitivity of the external force term is reduced to zero. Examples of design dependent pressure loading using the proposed method are shown satisfactory results.

References

Allaire G, Jouve F, Taoder AM (2004) Structural optimization using sensitivity analysis and a level-set method. J Comput Phys 194:363–393

Bendsøe MP, Kikuchi N (1988) Generating optimal topologies in structural design using a homogenization method. Computer Methods Appl Mech Eng 71:197–224

Bendsøe MP, Sigmund O (2004) Topology optimization, 2nd edn. Springer, Heidelberg

Bourdin B, Chambolle A (2003) Design-dependent loads in topology optimization. ESAIM: Control Optim Calc Var 9:19–48

Chen T-Y, Wu S-C (1998) Multiobjective optimal topology design of structures. Comput Mech 21:483–494

Chen B, Kikuchi N (2001) Topology optimization with design-dependent loads. Finite Elem Anal Des 37:57–70

Chickermane H, Gea HC (1996) Structural optimization using a new local approximation method. Int J Numer Methods Eng 39(5):829–846

Chickermane H, Gea HC (1997) Design of multi-component structural systems for optimal layout topology and joint locations. Eng Comput 13:235–243

Diaz A, Bendsøe MP (1992) Shape optimization of structures for multiple loading situations using a homogenization method. Struct Optim 4:17–22

Du J, Olhoff N (2004a) Topology optimization of continuum structures with design-dependent surface loading—part I: new computational approach for 2D problems. Struct Multidisc Optim 27:151–165

Du J, Olhoff N (2004b) Topology optimization of continuum structures with design-dependent surface loading—part II: algorithm and examples for 3D problems. Struct Multidisc Optim 27:166–177

Du J, Olhoff N (2007) Topological design of freely vibrating continuum structures for maximum values of simple and multiple eigenfrequencies and frequency gaps. Struct Multidisc Optim 34:91–110

Duysinx P, Bendsøe MP (1998) Topology optimization of continuum structures with local stress constraints. Int J Numer Method Eng 43:1453–1478

Fuchs MB, Shemesh NNY (2004) Density-based topologic design of structures subjected to water pressure using a parametric loading surface. Struct Multidisc Optim 28:11–19

Gea HC (1996) Topology optimization: a new micro-structural based design domain method. Comput Struct 61(5):781–788

Gea HC, Fu Y (1997) Optimal 3D stiffener design with frequency considerations. Adv Eng Softw 28:525–531

Hammer VB, Olhoff N (2002) Topology optimization of continuum structures subjected to pressure loading. Struct Multidisc Optim 19:85–92

Jung D, Gea HC (2004) Topology optimization of nonlinear structures. Finite Elem Anal Des 40:1417–1427

Luo J, Gea HC (1998) A systematic topology optimization approach for optimal stiffener design. Struct Optim 16(4): 280–288

Pedersen NL (2000) Maximization of eigenvalues using topology optimization. Struct Multidisc Optim 20:2–11

Rozvany GIN, Prager W (1979) A new class of structural optimization problems: optimal archgrids. Comput Methods Appl Mech Eng 19:127–150

Sigmund O, Clausen PM (2007) Topology optimization using a mixed formulation: an alternative way to solve pressure load problems. Comput Methods Appl Mech Eng 196:1874–1889

Suzuki K., Kikuchi N (1991) A homogenization method for shape and topology optimization. Comput Methods Appl Mech Eng 93:291–318

Tortorelli D, Michaleris P (1994) Design sensitivity analysis: overview and review. Inverse Probl Eng 1:71–105

Wang X, Wang MY, Guo D (2004) Structural shape and topology optimization in a level-set based framework of region representation. Struct Multidisc Optim 27(1–2):1–19

Yang XY, Xie YM, Steven GP (2005) Evolutionary methods for topology optimization of continuous structures with design dependent loads. Comput Struct 83:956–963